Available online at www.sciencedirect.com
SCIENCE DIRECT
C. R. Mecanique 333 (2005) 51–57
COMPTES RENDUS MECANIQUE
http://france.elsevier.com/direct/CRAS2B/

High-Order Methods for the Numerical Simulation of Vortical and Turbulent Flows

A symmetry-preserving Cartesian grid method for computing a viscous flow past a circular cylinder

Roel Verstappen, Marc Dröge

Research Institute of Mathematics and Computing Science, University of Groningen, P.O. Box 800, 9700 AV Groningen, The Netherlands

Available online 28 December 2004

Abstract

This article deals with a numerical method for solving the unsteady, incompressible Navier–Stokes equations in domains with arbitrarily-shaped boundaries, where the boundary is represented using the Cartesian grid approach. We introduce a novel cut-cell discretization which preserves the spectral properties of convection and diffusion. Here, convection is discretized by a skew-symmetric operator and diffusion is approximated by a symmetric, positive-definite coefficient matrix. Such a symmetry-preserving discretization conserves the kinetic energy (if the dissipation is turned off) and is stable on any grid. The method is successfully tested for an incompressible, unsteady flow around a circular cylinder at $Re = 100$. ***To cite this article: R. Verstappen, M. Dröge, C. R. Mecanique 333 (2005).***

Résumé

Une méthode de grille cartésienne préservant la symétrie pour le calcul d'un écoulement visqueux autour d'un cylindre circulaire. Cet article décrit une méthode numérique de résolution des équations de Navier–Stokes incompressibles instationnaires dans des domaines de géométries arbitraires. Nous partons d'une grille cartésienne, modifiée près de la frontière par une nouvelle méthode de découpage de maille, compatible avec les propriétés spectrales des opérateurs de convection et de diffusion. Ainsi, les termes de convection sont discrétisés avec un opérateur discret anti-symétrique (skew-symmetric) et les termes de diffusion sont approchés par un opérateur discret symétrique défini positif. Une telle discrétisation préservant la symétrie permet de conserver l'énergie cinétique (quand la viscosité est negligée) et elle est stable sur n'importe quelle grille. La méthode a été testée avec succès dans le cas de écoulement incompressible instationnaire autour d'un cylindre de section circulaire pour une valeur du nombre de Reynolds $Re = 100$. ***Pour citer cet article : R. Verstappen, M. Dröge, C. R. Mecanique 333 (2005).***

Keywords: Computational fluid mechanics; Cartesian grid method; Symmetry-preserving discretization

Mots-clés : Mécanique des fluides numérique ; Approximation de grille cartésienne ; Discrétisation préservant la symétrie

E-mail addresses: verstappen@math.rug.nl (R. Verstappen), marc@math.rug.nl (M. Dröge).

1631-0721/$ – see front matter
doi:10.1016/j.crme.2004.09.021

1. Introduction

This article deals with a numerical method for solving the unsteady, incompressible Navier–Stokes equations in domains with arbitrarily-shaped boundaries, where the boundary is represented using the Cartesian grid approach cf. [1–4]. The discretization of the convective and viscous fluxes through the faces of the irregular-shaped cells created by the intersection of the boundary with the Cartesian grid forms the primary difficulty in a Cartesian grid method. Away from the boundary, the simple structure of the Cartesian grid allows to retain much of the numerical techniques that have proven to be successful for flows in simple, grid-aligned domains. For such flows, we have proposed to compute numerical solutions of the Navier–Stokes equations in such a manner that the difference operators do have the same symmetry properties as the corresponding differential operators [5]. Applied to the incompressible Navier–Stokes equations, the symmetry-preserving discretization method yields a dynamical system of the form

$$\boldsymbol{\Omega}\frac{\mathrm{d}\boldsymbol{u}_h}{\mathrm{d}t} + \boldsymbol{C}(\boldsymbol{u}_h)\boldsymbol{u}_h + \boldsymbol{D}\boldsymbol{u}_h - \boldsymbol{M}^*\boldsymbol{p}_h = \boldsymbol{0}, \quad \boldsymbol{M}\boldsymbol{u}_h = \boldsymbol{0} \tag{1}$$

where $\boldsymbol{u}_h$ denotes the semi-discrete velocity vector, $\boldsymbol{p}_h$ stands for the discrete pressure, $\boldsymbol{\Omega}$ is a (positive-definite) diagonal matrix representing the sizes of the control volumes and $\boldsymbol{M}$ is the coefficient matrix of the discretization of the integral form of the law of conservation of mass. Here, the convective coefficient matrix $\boldsymbol{C}(\boldsymbol{u}_h)$ is skew symmetric like the underlying differential operator $(\boldsymbol{u}\cdot\nabla)$, i.e.

$$\boldsymbol{C}(\boldsymbol{u}_h) + \boldsymbol{C}(\boldsymbol{u}_h)^* = \boldsymbol{0} \tag{2}$$

and the discrete diffusive operator $\boldsymbol{D}$ is symmetric, positive definite like $-\nabla^2$. Mimicking crucial properties of differential operators forms in itself a motivation for discretizing them in a certain manner. We give it a concrete form by noting that the energy $\|\boldsymbol{u}_h\|^2 = \boldsymbol{u}_h^*\boldsymbol{\Omega}\boldsymbol{u}_h$ of any solution of (1) evolves according to

$$\frac{\mathrm{d}}{\mathrm{d}t}(\boldsymbol{u}_h^*\boldsymbol{\Omega}\boldsymbol{u}_h) \overset{(1)}{=} -\boldsymbol{u}_h^*\big(\boldsymbol{C}(\boldsymbol{u}_h) + \boldsymbol{C}(\boldsymbol{u}_h)^*\big)\boldsymbol{u}_h - \boldsymbol{u}_h^*(\boldsymbol{D}+\boldsymbol{D}^*)\boldsymbol{u}_h \overset{(2)}{=} -\boldsymbol{u}_h^*(\boldsymbol{D}+\boldsymbol{D}^*)\boldsymbol{u}_h$$

where the right-hand side is negative for all $\boldsymbol{u}_h \neq \boldsymbol{0}$ since $\boldsymbol{D}$ is a symmetric, positive-definite matrix. This implies that the semi-discrete system (1) is stable. Therefore a solution of (1) can be obtained on any grid. Note that the discrete pressure does not contribute to the evolution of the discrete energy because $((\boldsymbol{M}^*\boldsymbol{p}_h)^*\boldsymbol{u}_h) = (\boldsymbol{p}_h^*\boldsymbol{M}\boldsymbol{u}_h) = 0$.

In this article, the symmetry-preserving discretization method is generalized to a Cartesian grid method. To that end, the convective flux through irregularly shaped boundary cells is discretized such that the associated coefficient matrix $\boldsymbol{C}(\boldsymbol{u}_h)$ is skew symmetric and the diffusive matrix is symmetric, positive definite. The method is tested for an incompressible, unsteady flow around a circular cylinder at $Re = 100$.

2. Symmetry-preserving discretization

On nonuniform Cartesian grids various ways exist to discretize convective and diffusive operators. In this section, we will discuss a finite-volume discretization of these operators that preserves the symmetry.

2.1. Choice of the control volumes

To start, we will explain our choice of the control volumes (in two spatial dimensions for simplicity). We assume that the geometry is so well resolved on the grid that the boundary of the geometry can be approximated linearly in any cut grid cell. The part of the grid cell $[x_{i-1}, x_i] \times [y_{j-1}, y_j]$ that is open to fluid flow is denoted by $\Omega_{i,j}$. The discrete velocity $(u_{i,j}, v_{i,j})$ is staggered. The control volume for $u_{i,j}$ takes up the right half of $\Omega_{i,j}$ and the left half of $\Omega_{i+1,j}$. Here, we cut the open part of the grid cell $\Omega_{i,j}$ into two equal halves, by viewing $\Omega_{i,j}$ as if it is built out of (an infinite number of) horizontal line-segments that run from x_{i-1} to x_i if the line-segment is uncut

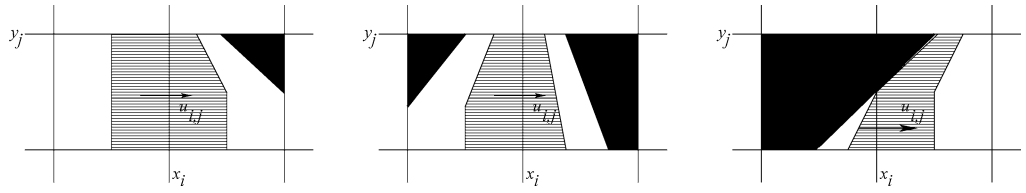

Fig. 1. Three control volumes for $u_{i,j}$. The parts that are not open to flow are colored black.

by a boundary, and from the boundary to either x_{i-1} or x_i (depending on which end lies in the fluid) if it is cut. Each line-segment is bisected and the half nearest to the grid line $x = x_i$ is taken. This definition is illustrated in Fig. 1 by means of three examples. The control volume for $v_{i,j}$ is defined in the same manner: its definition can be obtained from that of $u_{i,j}$ by exchanging x and y. For uncut cells, the control volumes are identical to those that were chosen in [6].

2.2. Conservation of mass

For an incompressible fluid, the integral of the normal component of the velocity over the surface of any grid cell is zero:

$$\bar{u}_{i,j} + \bar{v}_{i,j} - \bar{u}_{i-1,j} - \bar{v}_{i,j-1} = 0 \tag{3}$$

where the mass fluxes through the faces are defined by

$$\bar{u}_{i,j} = \int_{y_{j-1}}^{y_j} u(x_i, y, t)\delta(x_i, y)\,\mathrm{d}y \quad \text{and} \quad \bar{v}_{i,j} = \int_{x_{i-1}}^{x_i} v(x, y_j, t)\delta(x, y_j)\,\mathrm{d}x \tag{4}$$

Here, the fluid domain is indicated by a function $\delta(x, y)$, which equals one inside the fluid and zero outside. Note, the combination (3), (4) does not yet contain a discretization error, since the integrals in (4) are exact.

2.3. Skew-symmetric discretization of convection

As mass and momentum are transported at equal velocity, we will use (4) to discretize the velocity at which momentum is transported. Thus, the momentum flux through a surface S is approximated by

$$\int_S u\boldsymbol{u}\cdot\boldsymbol{n}\,\mathrm{d}S \approx u_S \int_S \boldsymbol{u}\cdot\boldsymbol{n}\,\mathrm{d}S$$

where u_S denotes a characteristic value of u at the surface S. At this stage, the integral in the right-hand side (that is the mass flux through S) is not approximated. The transport of momentum through the faces of a control volume for $u_{i,j}$ becomes approximately

$$|\Omega_{i+1/2,j}|\frac{\mathrm{d}u_{i,j}}{\mathrm{d}t} + u_{i+1/2,j}\bar{u}_{n\,i+1/2,j} + u_{i,j+1/2}\bar{v}_{i+1/2,j} - u_{i-1/2,j}\bar{u}_{n\,i-1/2,j} - u_{i,j-1/2}\bar{v}_{i+1/2,j-1} \tag{5}$$

where $|\Omega_{i+1/2,j}|$ denotes the size of the control volume for $u_{i,j}$. The non-integer indices in (5) refer to the faces of the control cell for $u_{i,j}$. For example, $u_{i+1/2,j}$ stands for a characteristic u-velocity at the interface between the control volumes for $u_{i,j}$ and $u_{i+1,j}$, and $\bar{v}_{i+1/2,j}$ denotes the (exact) mass flux through the common boundary of the control volumes for $u_{i,j}$ and $u_{i,j+1}$, etc. Note that the mass flux through a part of the interface between the control volumes for $u_{i,j}$ and $u_{i+1,j}$ need not be aligned with u. Therefore, it is denoted by $\bar{u}_n$ and not by $\bar{u}$; see also Fig. 2.

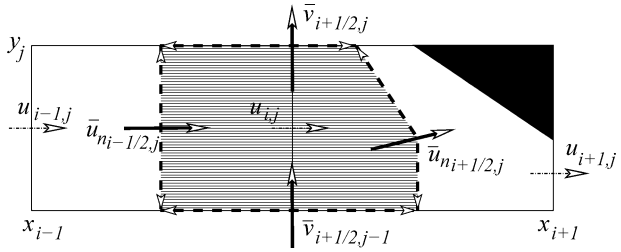

Fig. 2. Mass flux through the boundary of the control volume for $u_{i,j}$.

The velocity at a control face is approximated by the average of the velocity at both sides of it:

$$u_{i+1/2,j} = \frac{1}{2}(u_{i+1,j} + u_{i,j}) \quad \text{and} \quad u_{i,j+1/2} = \frac{1}{2}(u_{i,j+1} + u_{i,j}) \tag{6}$$

In addition to the set of equations for the u-component of the velocity $\boldsymbol{u} = (u, v)$, there is an analogous set for the v-component. We conceive Eq. (5) together with the interpolation rule (6) as an expression for the velocities, where the mass fluxes form the coefficients. Thus, we can write the discretization (5)+(6), together with an analogous set for the v-component, in matrix-vector notation as

$$\boldsymbol{\Omega}\frac{\mathrm{d}\boldsymbol{u}_h}{\mathrm{d}t} + \boldsymbol{C}(\bar{\boldsymbol{u}})\boldsymbol{u}_h$$

where the coefficient matrix $\boldsymbol{C}(\bar{\boldsymbol{u}})$ depends on the mass fluxes through the control faces. Note that we make liberal use of its name: $\boldsymbol{C}$ was viewed as a function of the discrete velocity $\boldsymbol{u}_h$ in the introductory section, whereas $\boldsymbol{C}$ is a function of exact mass fluxes here.

In the introductory section, we saw that (for $\boldsymbol{D} = \boldsymbol{0}$) the spatial discretization (1) conserves the energy $\boldsymbol{u}_h^*\boldsymbol{\Omega}\boldsymbol{u}_h$ if and only if the convective coefficient matrix $\boldsymbol{C}(\bar{\boldsymbol{u}})$ is skew symmetric. Hence, the spatial discretization is stable when $\boldsymbol{C}(\bar{\boldsymbol{u}})$ is skew symmetric. The matrix $\boldsymbol{C}(\bar{\boldsymbol{u}}) - \mathrm{diag}(\boldsymbol{C}(\bar{\boldsymbol{u}}))$ is skew symmetric if and only if the weights in the interpolation of u (and v) to the control faces are constant, as in Eq. (6). Therefore we use (6) also on nonuniform grids. To make $\boldsymbol{C}(\bar{\boldsymbol{u}})$ skew symmetric, the interpolation rule for $\bar{u}$ and $\bar{v}$ is determined by the requirement that the diagonal of $\boldsymbol{C}(\bar{\boldsymbol{u}})$ has to be zero. By substituting the interpolation rule (6) into (5) we obtain the diagonal coefficient

$$\frac{1}{2}(\bar{u}_{ni+1/2,j} + \bar{v}_{i+1/2,j} - \bar{u}_{ni-1/2,j} - \bar{v}_{i+1/2,j-1})$$

This expression is zero if the mass is conserved in the grid cells and the mass fluxes in (5) are interpolated to the control faces with weights one half:

$$\bar{u}_{ni+1/2,j} = \frac{1}{2}(\bar{u}_{i+1,j} + \bar{u}_{i,j}) \quad \text{and} \quad \bar{v}_{i+1/2,j} = \frac{1}{2}(\bar{v}_{i+1,j} + \bar{v}_{i,j}) \tag{7}$$

The interpolation of $\bar{u}_{ni+1/2,j}$ is illustrated in Fig. 3(left). The mass flux $\bar{u}_{ni+1/2,j}$ through the right-hand face of the control volume for $u_{i,j}$ is written as the average of the mass flux at both sides: $\bar{u}_{ni+1/2,j} = \frac{1}{2}(\bar{u}_{\mathrm{left}} + \bar{u}_{\mathrm{right}})$, where we take the flux through the face $x = x_i$ for the left-hand side, that is $\bar{u}_{\mathrm{left}} = \bar{u}_{i,j}$. The right-hand contribution is approximated by the sum of the mass flux through the hypotenuse of the triangle that is not open to the flow and the mass flux through the open part of the face $x = x_{i+1}$, i.e. $\bar{u}_{\mathrm{right}} = 0 + \bar{u}_{i+1,j}$. The flux $\bar{v}_{i+1/2,j}$ is also seen as the sum of a left- and right-hand contribution, $\bar{v}_{i+1/2,j} = \bar{v}_{\mathrm{left}} + \bar{v}_{\mathrm{right}}$, with $\bar{v}_{\mathrm{left}} = \frac{1}{2}\bar{v}_{i,j}$ and $\bar{v}_{\mathrm{right}} = \frac{1}{2}\bar{v}_{i+1,j}$, see Fig. 3(right).

Obviously, the mass flux $\bar{\boldsymbol{u}}$ need be expressed in terms of the discrete velocity vector $\boldsymbol{u}_h$ to close the discretization. The coefficient matrix $\boldsymbol{C}(\bar{\boldsymbol{u}})$ becomes a function of the discrete velocity $\boldsymbol{u}_h$ then: $\boldsymbol{C}(\boldsymbol{u}_h) = \boldsymbol{C}(\bar{\boldsymbol{u}}(\boldsymbol{u}_h))$. The

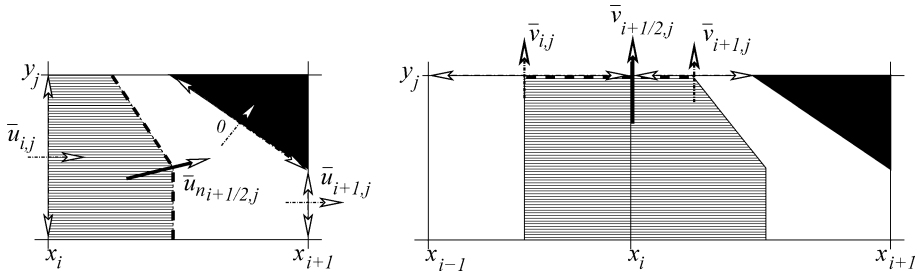

Fig. 3. Illustration of the interpolation of the mass flux $\bar{u}_{n\,i+1/2,j}$ (left-hand) and $\bar{v}_{i+1/2,j}$ (right-hand). Here, the black triangle is not open to flow. The dashed line represents the cell face.

matrix $\boldsymbol{C}(\boldsymbol{u}_h)$ is skew symmetric for any relation between $\bar{\boldsymbol{u}}$ and $\boldsymbol{u}_h$. We relate the mass fluxes $\bar{\boldsymbol{u}}$ to the discrete velocity $\boldsymbol{u}_h$ by means of:

$$\bar{u}_{i,j} = u_{i,j} \int_{y_{j-1}}^{y_j} \delta(x_i, y)\,\mathrm{d}y \quad \text{and} \quad \bar{v}_{i,j} = v_{i,j} \int_{x_{i-1}}^{x_i} \delta(x, y_j)\,\mathrm{d}x. \tag{8}$$

Substituting these approximations into Eq. (3) gives the discrete continuity constraint, which confines the discrete velocity to $\boldsymbol{M}\boldsymbol{u}_h = \boldsymbol{0}$.

2.4. Discretization of diffusion

In the continuous case diffusion corresponds to a symmetric, positive definite operator. We want this property to hold also for the discrete operator $\boldsymbol{D}$ in Eq. (1). To that end, the diffusive flux through the interface S between the control volumes of $u_{i-1,j}$ and $u_{i,j}$ may be approximated in a common way:

$$\frac{1}{Re}\int_S \nabla u \cdot \boldsymbol{n}\,\mathrm{d}s \approx \frac{u_{i-1,j} - u_{i,j}}{Re|\boldsymbol{n}_S|}|S| \tag{9}$$

where the length of the vector $\boldsymbol{n}_S$ is approximated in terms of the size of the face S and sizes of the control volumes for $u_{i-1,j}$ and $u_{i,j}$. The diffusive flux through the other faces of the control cell for $u_{i,j}$ is discretized similarly. The resulting coefficient matrix $\boldsymbol{D}$ is symmetric and positive definite.

3. Flow over a circular cylinder

The Cartesian grid method (outlined in Section 2) is applied to compute the unsteady flow around a circular cylinder at $Re = 100$, where the Reynolds number Re is based upon the diameter of the cylinder and the free stream velocity. This flow has served as a test case for various numerical approaches. In this section, we will compare our results with those in [7] and [8]. Kravchenko et al. [7] considered the flow past a circular cylinder to evaluate their Galerkin B-spline method. Persillon and Braza [8] studied the test case by means of a second-order, curvilinear, finite-volume method. Experimental data can be found in [9] and the references therein.

To confine the flow domain, fictitious boundaries are necessary (sufficiently) far away from the cylinder. We take the inflow boundary at four diameters upstream from the cylinder. The inflow condition reads $u = 1$, $v = 0$. The lateral boundaries are taken 8 diameters apart. At these boundaries the normal derivatives of the components of the velocity are set equal to zero. The outflow is located at 10 diameters past the cylinder. Also at the outflow, Neumann conditions are applied. Computations have been performed on four grids consisting of 100×120, 150×180,

Table 1
Comparison with other simulations and experiments. When given, the drag coefficient is written as the sum of the pressure drag and the viscous drag. The experimental data is taken from [9] and the references therein

	St	$C_{D,p}$	$C_{D,f}$	C_D	$\max C_L$	θ_{sep}
Present	0.165	0.93	0.31	1.24	0.30	117
[7]	0.164	0.97	0.34	1.31*	0.314	117.4
[8]	0.165			1.253	0.38	113.5
Exp. [10]		1.0	0.3	1.3		
Experiment	0.164–0.165			1.24–1.26 [11]		122 [12]

* Note: [7] gives the $\max C_D$. In our case, $\max C_D$ is 0.02 higher than mean C_D.

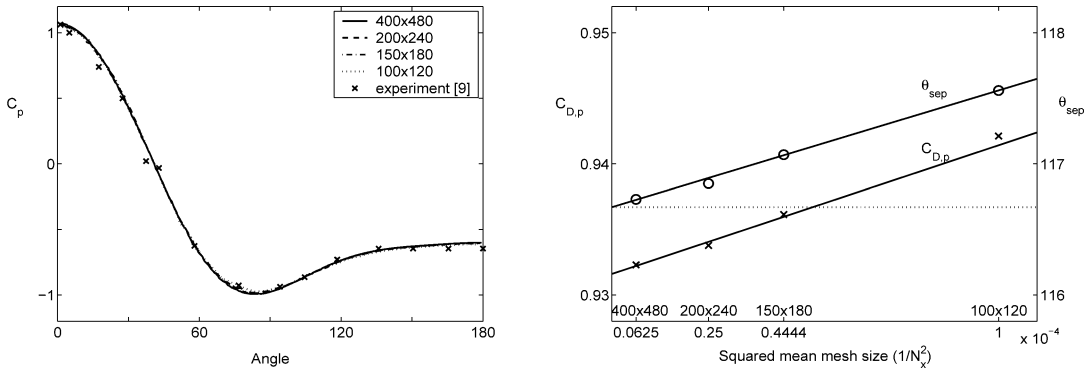

Fig. 4. (Left) A comparison between experiment and simulation: the pressure distribution at the surface of the cylinder, as function of the angle. (Right) The separation angle θ_{sep} and pressure drag $C_{D,p}$ as function of the square of the mean mesh size.

200×240 and 400×480 points (in lateral and streamwise direction) respectively. The time-integration is performed as in [5].

Table 1 shows a comparison of bulk quantities as obtained from our fine-grid simulation with those of the references mentioned above. The good agreement with the other numerical simulation techniques as well as with the physical experiments confirms the correct behavior of the present approach and shows that the symmetry-preserving Cartesian grid method forms a good alternative for boundary-fitted structured and boundary-fitted unstructured methods. Fig. 4(left) displays the pressure distribution at the surface of the cylinder as obtained with the symmetry-preserving Cartesian grid method. At all four grids the numerical result is in good agreement with an experimentally determined pressure distribution. To study the convergence of the symmetry-preserving scheme upon grid refinement, the pressure drag $C_{D,p}$ and the separation angle θ_{sep} are shown as function of the square of the mean mesh size in Fig. 4(right). The figure shows that $C_{D,p}$ and θ_{sep} are (approximately) linear functions of the square of the mean mesh size. Hence, we may conclude that the scheme is second-order.

References

[1] J. Purvis, J. Burkhalter, Prediction of critical Mach number store configurations, AIAA J. 17 (1979) 1170–1177.
[2] M. Berger, R. LeVeque, An adaptive Cartesian mesh algorithm for the Euler equations in arbitrary geometries, in: Proc. 9th AIAA. CFD Conf., Buffalo, NY, 1991, pp. 1–7.
[3] T. Ye, R. Mittal, H.S. Udaykumar, W. Shyy, An accurate Cartesian grid method for viscous incompressible flow with complex boundaries, J. Comp. Phys. 156 (1999) 209–240.
[4] D. Calhoun, R.J. LeVeque, A Cartesian grid finite volume method for the advection–diffusion equation in irregular geometries, J. Comp. Phys. 157 (2000) 143–180.

[5] R.W.C.P. Verstappen, A.E.P. Veldman, Symmetry-preserving discretization of turbulent flow, J. Comp. Phys. 187 (2003) 343–368.
[6] F.H. Harlow, J.E. Welsh, Numerical calculation of time-dependent viscous incompressible flow of fluid with free surface, Phys. Fluids 8 (1965) 2182–2189.
[7] A.G. Kravchenko, P. Moin, K. Shariff, B-spline method and zonal grids for simulations of complex turbulent flows, J. Comp. Phys. 151 (1999) 757–789.
[8] H. Persillon, M. Braza, Physical analysis of the transition to turbulence in the wake of a circular cylinder by three-dimensional Navier–Stokes simulation, J. Fluid Mech. 365 (1998) 23–88.
[9] M.M. Zdravkovich, Flow Around Circular Cylinders. Vol. 1: Fundamentals, Oxford University Press, 1997.
[10] R.D. Henderson, Details of the drag curve near the onset of vortex shedding, Phys. Fluids 7 (1995) 2102–2104.
[11] D.J. Tritton, Experiments on the flow past a circular cylinder at low Reynolds numbers, J. Fluid Mech. 6 (1959) 547–567.
[12] H.G. Dimopoulos, T.J. Hanratty, Velocity gradients at the wall for flow around a cylinder for Reynolds numbers between 60 and 360, J. Fluid Mech. 33 (1968) 303–319.